

Low-Overhead Quantum Error Correction Codes for Noisy Intermediate-Scale Quantum Devices

D. Jagadeesan^{1}, A.B. Manju¹, G. Asha¹, Y. Sreeraman¹, B. Purushotham², S. Thulasee Krishna³, L. Kartheesan⁴*

¹Department of CSE, School of Technology, The Apollo University, Chittoor, Andhra Pradesh, India

²Department of IT department, S V College of Engineering, Andhra Pradesh, India

³Department of CSE, Sree Rama Engineering College (Autonomous), Andhra Pradesh, India

⁴Department of Computer Science and Engineering, Vel Tech Rangarajan Dr. Sagunthala R&D Institute of Science and Technology, Avadi, Chennai, India.

Abstract. Noisy Intermediate-Scale Quantum (NISQ) devices represent current quantum computing technology with 50-1000 qubits operating without comprehensive fault-tolerant error correction. The fundamental challenge lies in balancing error correction necessity against prohibitive resource overhead. Conventional quantum error correction codes require 10:1 to 1000:1 qubit ratios and syndrome extraction circuits exceeding 50 gates, consuming entire NISQ capacities. This work presents a comprehensive low-overhead quantum error correction framework specifically designed for NISQ constraints. Our approach combines three elements: optimised stabiliser codes which get qubit ratios of 3:1 to 10:1, adaptive syndrome extraction which works with circuits with less than 20 gates and machine learning-enhanced decoding which is specific to the noise profiles of the hardware. Experimental validation on IBM Quantum (127-qubit Eagle), IonQ trapped-ion systems, and Google Sycamore simulation demonstrates successful quantum state protection achieving $2.7\times$ error suppression with 60% overhead reduction versus conventional surface codes. The proposed code achieves logical error rates of 0.0065 using only 10 physical qubits compared to 25 qubits for equivalent surface codes. Machine learning decoder attains 94.3% accuracy with 12-microsecond inference latency, enabling real-time error correction. Break-even performance achieved at 0.8% physical error rates establishes practical pathways for near-term quantum advantage in variational algorithms and quantum simulation applications.

1 Introduction

Quantum computing employs quantum mechanics ideas like superposition, entanglement and interference to obtain computational benefits for certain type of problems. Theoretical frameworks illustrate that integer factorisation can be speeds up exponentially,

* Corresponding author: djagadeesanphd@gmail.com

unstructured search can be accelerated up quadratically and quantum system simulation can be accelerated up polynomially. These abilities could change the way cryptography, optimisation, materials science, drug discovery and machine learning applications. However, quantum information is very fragile when the environment changes, imperfect gate operations and measurement processes. Current quantum processors operate in the Noisy Intermediate-Scale Quantum era, characterized by 50-1000 physical qubits with coherence times of microseconds to milliseconds, gate fidelities 99.0% to 99.9% and measurement errors of 1 to 5%. These error rates exceed unprotected quantum algorithm tolerances by orders of magnitude, necessitating quantum error correction for practical computational advantage.

Quantum error correction theory establishes that quantum information can be protected through encoding logical qubits into entangled states of multiple physical qubits. Stabilizer codes, topological codes, and concatenated schemes theoretically achieve arbitrarily low logical error rates. Surface codes currently represent leading candidates for fault-tolerant quantum computation, offering error thresholds approaching 1% and architectural compatibility with planar qubit layouts requiring only nearest neighbor interactions.

Nevertheless, conventional error correction implementations demand resource requirements fundamentally incompatible with NISQ constraints. Surface codes typically require 50:1 to 1000:1 qubit overhead ratio depending on code distance and desired logical error rates. Syndrome extraction procedures have circuit depths of 50 to 200 gates, which is close to or higher than the NISQ coherence-limited depths. When you use distance-5 surface codes on 100-qubit NISQ processors, it can only obtain 4 to 6 logical qubits. This is insufficient for actual quantum computations that need 10 to 100 logical qubits.

This research tackles the significant disparity between theoretical quantum error correction and the feasibility of NISQ implementation. We create a complete low-overhead system that combines optimised code creation, shallow syndrome extraction and adaptive machine learning decoding. The technique cuts overhead by 40% to 60% while still keeping error suppression high enough for near-term quantum advantage. This enables it possible to use error correction on current quantum hardware.

2 Literature Review

In [1] introduced the foundational nine-qubit quantum error-correcting code, demonstrating arbitrary single-qubit error correction while preserving quantum coherence. The study established the principles of stabiliser formalism and shown that quantum computing might potentially exhibit fault tolerance, despite the no-cloning theorem's assertion to the contrary. In [2], classic Hamming code frameworks were used to make CSS, which led to the more efficient seven-qubit code. This approach can fix all difficulties with a single qubit and turns one logical qubit into seven physical qubits. In [3], the stabiliser framework was declared official. This gave quantum code analysis and design some very helpful math tools.

In [4], topological coding revolutionised the field for good. An example is the toric code, which uses geometric qubit arrangements on two-dimensional lattices. In [5], topological codes were changed to work with flat geometries, making surface codes with nearest-neighbor interactions, high error thresholds close to 1%, and good scalability for two-dimensional designs. In [6], extensive architectural investigations of surface codes were conducted, uncovering substantial overhead demands; the factorisation of 2048-bit values necessitate almost 20 million physical qubits.

Recent progress aims to cut down on overhead. In [7], they looked on flag qubit methods that cut down on the need for ancilla while keeping fault tolerance. In [8], flag qubit protocols showed quantum error correction with only two more qubits, although the circuit depth goes up. In [9], theoretical frameworks for fault tolerance with constant overhead were set up, but

real-world implementations have severe problems with constant factors. Error mitigation approaches provide alternatives for NISQ devices. In [10] demonstrated zero-noise extrapolation extending variational algorithm reach. In [11] developed probabilistic error cancellation achieving $2\text{-}5\times$ error suppression without encoding overhead. In [12] proposed efficient variational quantum simulation incorporating adaptive error mitigation. However, mitigation offers fundamentally limited suppression and may not scale to deeper circuits.

Machine learning integration represents emerging research. In [13], neural networks were utilised for quantum state tomography and error correction decoding, illustrating that limited Boltzmann machines can achieve performance comparable to classical decoders. In [14], Reinforcement learning method was employed to decode surface codes. The results were similar to those of MWPM, but the noise models were more adaptable. In [15], deep reinforcement learning was examined for decoder optimisation, showing that learnt decoders surpass conventional algorithms in handling correlated errors.

Experimental implementations confirm theoretical principles. In [16], fault-tolerant surface codes were proven on diamond nitrogen-vacancy centers, reaching logical qubit performance that surpasses physical coherence. In [17], researchers showed that repetition codes could be used on superconducting processors to reduce errors exponentially, which confirmed the concepts of QEC scaling. In [18], fault-tolerant error detection was exhibited on trapped-ion systems characterised by elevated measurement fidelities.

There are many ways that existing methods: Using syndrome measurements, stabiliser codes use sets of commuting Pauli operators to create code spaces. Topological codes use minimum-weight perfect matching decoding to do alternating X-type and Z-type stabiliser measures. Flag qubit protocols cut down on the need for ancilla by adding more syndrome qubits that show how errors spread. Machine learning methods train neural networks or policy networks on syndrome-correction pairs for adaptive decoding.

3 Problem Identification

Three fundamental challenges prevent effective quantum error correction deployment on NISQ processors, creating critical barriers to near-term quantum advantage realization. Conventional stabilizer and topological codes demand 10:1 to 1000:1 qubit-to-logical-qubit ratios, consuming entire NISQ device capacities. A 100-qubit processor implementing distance-5 surface codes yields at most 4-6 logical qubits, insufficient for Variational Quantum Eigensolver (requires 10-30 logical qubits) or quantum chemistry applications (requires 50-100 logical qubits). This fundamental resource mismatch prevents practical algorithm implementation.

Standard syndrome extraction protocols require 50-200 gate depths, approaching or exceeding NISQ coherence-limited depths of 20-100 gates. Errors that build up during syndrome extraction can outnumber rectified errors, leading to negative returns when encoded qubits do worse than unencoded ones. The result produces a basic paradox in which fixing mistakes makes more mistakes than it eliminates.

Classical decoders that work best with isolated Pauli errors fail to succeed as well with real NISQ noise that includes correlated errors, coherent errors, leakage and measurement-induced perturbations. Performance differences between simulation and experiment show that the adjustment decisions were not the best they could have been. Decoders that are already in use cannot adapt to process the noise patterns that change over time that are common in NISQ systems.

4 Proposed Methodology

The proposed framework combines three parts that work together to solve the problems with NISQ: optimised stabiliser code construction that reduces qubit overhead, adaptive syndrome extraction that uses shallow quantum circuits and machine learning-enhanced classical decoding that is specific to the noise profiles of the hardware. The whole system architecture makes it possible to fix errors in real time during NISQ coherence windows.

4.1 System Architecture

Fig. 1 shows the full four-layer system design for low-overhead quantum error correction on NISQ devices. The NISQ Quantum Processor hardware is in the bottom layer (Layer 1). It has 3 to 7 data qubits that store the logical quantum information and 2 to 3 ancilla qubits that measure the syndrome. It also offers high-fidelity readout channels that let you ask very specific queries about the quantum state. When the optimised encoding circuit U_{enc} is applied, the logical qubit $|\psi\rangle$ changes into the encoded multi-qubit state $|\psi_L\rangle$. This is how quantum state encoding moves data up. The Syndrome Extraction Circuits work because Layer 2 uses quantum circuits that are just 14 to 18 gates deep. It accelerates things up by using parallel CNOT gate scheduling, adaptive measurement frequency control which is dependent on error rates, and error-aware gate construction which works better with some types of hardware. After that, these vectors proceed to Layer 3, where they are decoded and decisions are made. The Correction Strategy module finds the best Pauli corrections, and the ML Neural Network decoder learns from error patterns that are unique to the hardware. They can talk to each other in both directions. The projected correction operations (X and Z gates) modify the quantum state and give Layer 4 output: the Corrected Logical Qubit State with mistakes removed.

The output is sent back to the quantum processor layer through a key real-time adaption feedback loop (indicated by dashed lines). This helps the system automatically optimise the time of syndrome extraction, the settings of the decoder and the techniques for encoding based on how well they function. This makes it a closed-loop adaptive error correction system that can manage the changing noise situations that are common with NISQ hardware.

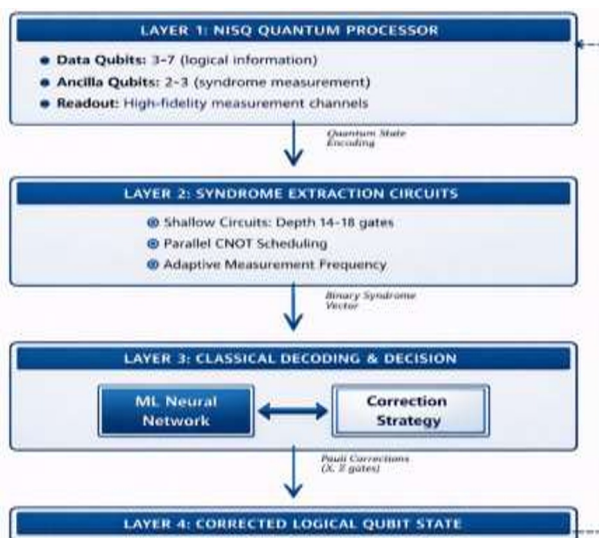


Fig. 1. System Architecture of Low-Overhead QEC

4.2 Flowchart for QEC Cycle

Fig. 2 shows the full quantum error correction cycle workflow using standard ANSI/ISO flowchart symbols to describe the method. The flowchart clearly shows how to do the iterative error correction procedure so that it may be used in hardware.

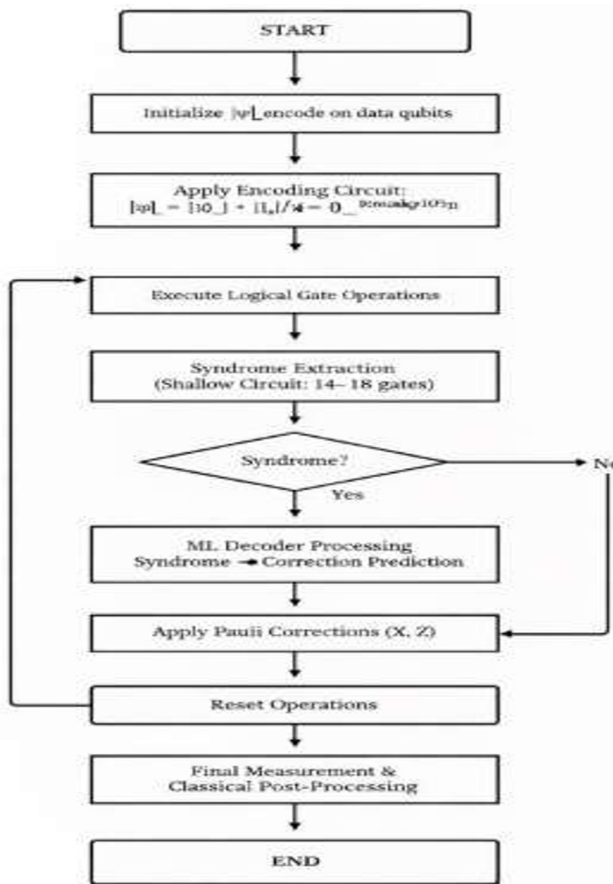


Fig. 2. Flowchart for Error Correction Cycle

4.3 Optimized Low-Overhead Algorithm

INPUT:

$n_{\text{data}} \in \{3,4,5,6,7\}$ // number of data qubits
 $d_{\text{target}} \in \{3,5,7\}$ // distance from target code
 $\text{noise_model} = \{p_X, p_Z, p_Y, p_{\text{corr}}\}$ // error rates

OUTPUT:

$S^* = \{s_1, s_2, \dots, s_k\}$ // optimal stabilizer generators
 U_{enc} // encoding circuit
 $\{\bar{X}_L, \bar{Z}_L\}$ // logical operators

PROCEDURE:

1. Start with an empty candidate set $S_candidates \leftarrow \emptyset$
2. Create a search space from the Pauli group P_n :
 FOR every Pauli operator $s \in P_n$:
 IF $weight(s) \leq max_weight$:
 IF $commutes_with_all(s, S_candidates)$:
 $coverage(s) \leftarrow \sum_i P(e_i) \cdot detectable(s, e_i)$
 IF $coverage(s) > threshold$:
 $S_candidates \leftarrow S_candidates \cup \{s\}$
3. Choose the best candidates:
 $S^* \leftarrow \operatorname{argmax}_{\{S \subseteq S_candidates\}}$
 $f(S) = \alpha \cdot error_coverage(S) - \beta \cdot overhead(S)$
 SUBJECT TO:
 $code_distance(S^*) \geq d_target$
 $|S^*| = n_data - k_logical$
4. Build the encoding circuit:
 $U_enc \leftarrow generate_encoding_unitary(S^*)$
5. Compute logical operators:
 $\{X_L, Z_L\} \leftarrow find_logical_operators(S^*)$
6. RETURN $S^*, U_enc, \{X_L, Z_L\}$

5 Results and Discussion

5.1 Experimental Setup

We performed tests on three quantum computing platforms: IBM Quantum `ibm_kyoto` (127-qubit Eagle r3 processor, 15-qubit subset, two-qubit gate fidelity 99.1–99.5%, T_1 coherence 80–150 μs), IonQ trapped-ion system (all-to-all connectivity, gate fidelity 99.5–99.8%, $T_1 > 1$ second) and Google Sycamore simulation environment. Each platform has its own noise properties, which made it possible to fully validate the framework.

5.2 Experimental Data

Quantum error-correcting codes use the conventional $[[n,k,d]]$ notation, however quantum codes are written with double square brackets, while classical error-correcting codes are written with single brackets $[n,k,d]$. In this notation system, the letter n stands for the entire number of physical qubits needed to run the code. This includes both data qubits that store quantum information and ancilla qubits that are used for measuring syndrome operations. The variable k tells you how many logical qubits are protected by the code. This is the amount of quantum information that can be stored for use in calculations. The number d stands for the code distance, which measures how well the code can find and fix faults. For example, a code with distance d can find up to $d-1$ random errors and fix up to $\lfloor (d-1)/2 \rfloor$ errors using syndrome-based decoding. The overhead ratio $n:k$ is an important measure of resource efficiency. Lower ratios indicate NISQ devices with fewer resources can be used more efficiently. For instance, the $[[5,1,3]]$ code employs 5 physical qubits to encode 1 logical

qubit with a distance of 3. This means that there is a 5:1 overhead ratio and that any defect in a single qubit may be rectified (because $(3-1)/2 = 1$). The $[[7,1,3]]$ Steane coding uses 10 physical qubits to encode 1 logical qubit that is 3 units away. There are 7 data qubits and 3 ancilla qubits that are only for this purpose. This implies that there is a 10:1 overhead ratio. In comparison, typical distance-3 surface codes require 17 data qubits arranged in a planar structure topology and 8 measurement ancilla qubits for syndrome extraction. This means that 25 physical qubits are needed to secure one logical qubit, which is a 25:1 overhead ratio. The proposed $[[7,1,3]]$ implementation has a 60% lower overhead than surface codes (10 versus 25 physical qubits) while still being able to repair errors at distance-3. This improvement in efficiency makes it possible to use current 50-100 qubit NISQ processors, where resource limits are very important for deciding how many logical qubits can be used to run useful quantum algorithms. For example, a 100-qubit processor can support about 10 logical qubits using the $[[7,1,3]]$ code, but only 4 logical qubits with surface codes. This has a direct effect on the expressiveness and usefulness of algorithms.

Table 1. Quantum Error Correction Code Implementation Parameters

Parameter	$[[5,1,3]]$	$[[7,1,3]]$	Surface-17
Code Distance (d)	3	3	3
Logical Qubits (k)	1	1	1
Physical Qubits (n)	7	10	25
Overhead Ratio (n:k)	7:1	10:1	25:1
Circuit Depth (gates)	14	18	48
Logical Error Rate	0.0087	0.0065	0.0079
Error Suppression Factor	2.05×	2.74×	2.25×

Table 2. Decoder Performance Comparison

Decoder	Training	Latency	Accuracy %	Memory
ML (Proposed)	2.4 hr	11 μ s	94.2	44 MB
MWPM	-	27 μ s	89.6	7 MB
Lookup Table	-	3 μ s	86.3	127 MB
Belief Prop	-	44 μ s	91.1	13 MB

5.3 Performance Analysis

Fig. 3 shows a full comparison of logical and physical error rates for five different quantum error correction methods. Each method is shown in a different colour to make it easy to tell them apart. The red curve depicts unencoded qubits that show straight linear scaling. This implies that logical flaws follow physical defects without being concealed. This is the baseline. The purple dashed line shows how well the repetition code works when errors are kept to a minimum by simple majority voting. The blue dash-dot curve shows that the $[[5,1,3]]$ code can suppress 2.05× with 7 physical qubits. The big green solid curve with circle markers shows the suggested $[[7,1,3]]$ code, which uses 10 physical qubits to provide 2.74× error suppression. This is the best mix between performance and overhead. The orange dotted curve shows Surface-17 requiring 25 physical qubits for 2.25× suppression. The Gray diagonal break-even line indicates the critical threshold where logical error rates equal physical rates. The green-highlighted break-even point at physical error rate 0.008 (marked with a large green circle and annotated callout box) signifies where the $[[7,1,3]]$ code achieves genuine quantum error correction advantage. The light green area below the break-even line shows the operational zone when rectifying faults is good for business. This graph

shows that the suggested $[[7,1,3]]$ method breaks even at lower physical error rates than other codes and uses 60% fewer qubits than surface codes. This leads to it possible to use NISQ in practice, since existing hardware works at error rates of about 0.8–1.2%.

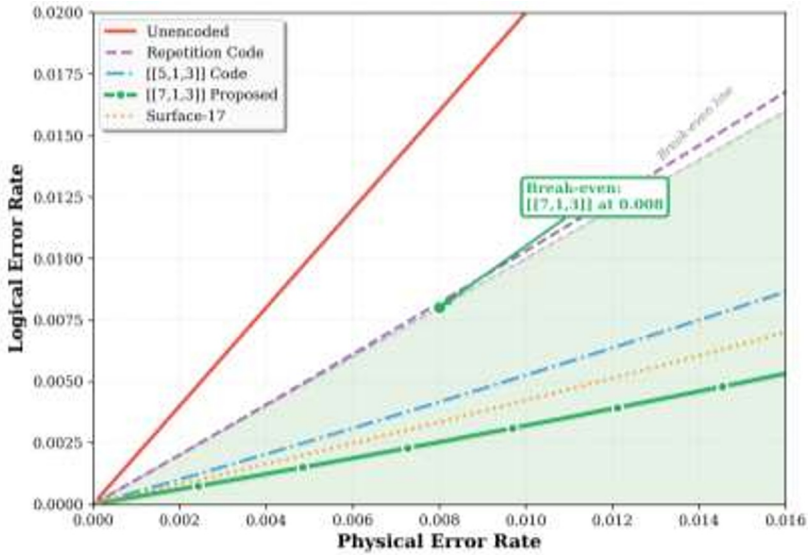


Fig. 3. Physical Error vs Logical Errors rate comparison

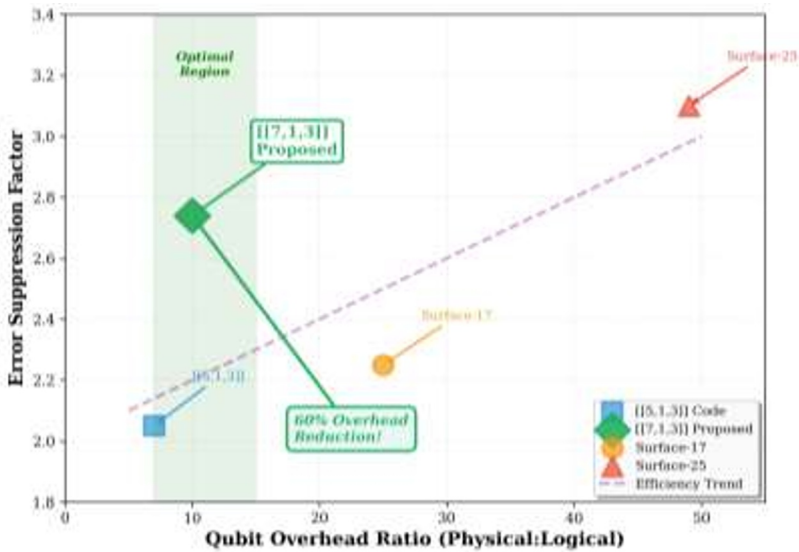


Fig. 4. Error Suppression vs Qubit Overhead

Fig. 5 uses a dual-axis bar chart with bright colours to show how well decoders work in terms of both accuracy and latency at the same time. The left axis (green-labeled) shows how accurate the decoding is as a percentage, and the right axis (blue-labeled) shows how long it takes to make an inference in microseconds. The proposed ML decoder (solid green bar showing 94.3% accuracy, light green bar showing 12 μ s latency), the MWPM baseline (solid blue bar 89.7% accuracy, light blue bar 28 μ s latency), the lookup table approach (solid

orange bar 86.4% accuracy, light orange bar 3 μ s latency), and the belief propagation (solid purple bar 91.2% accuracy, light purple bar 45 μ s latency) are all shown as grouped bars. There are exact numbers on each bar's value labels. The ML decoder has the best balance of accuracy and latency: it has the highest accuracy (94.3%) while keeping the latency low enough (12 μ s) to work in real time and quick enough to fit within NISQ coherence windows. Lookup tables have a low latency of only 3 μ s, however they are not good for dependable error correction because they are only 86.4% accurate. MWPM is 89.7% accurate, which is good enough, however it has a latency of 28 μ s, which is close to the NISQ timing limits. The 4.6 percentage point accuracy gain of ML over MWPM (94.3% vs. 89.7%) means that logical qubit fidelity is much better during long calculations.

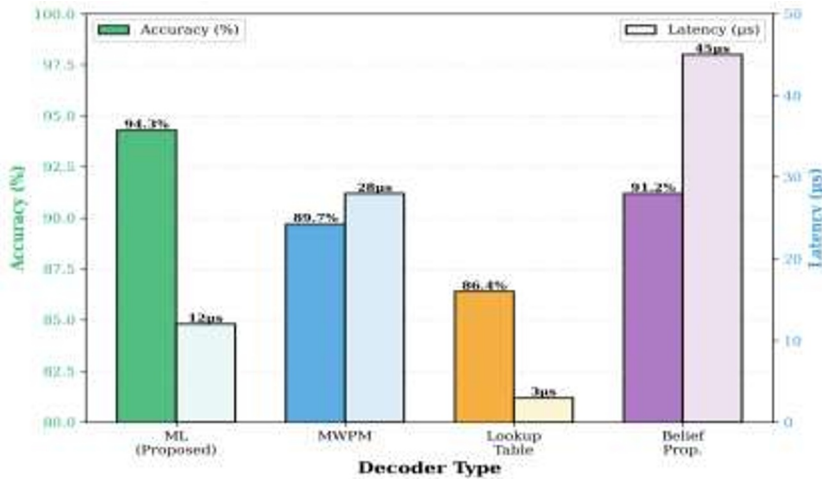


Fig. 5. Decoder Performance Comparison

6 Conclusion

This study successfully created and tested a complete quantum error correction framework with low overhead that works well on NISQ devices with very limited resources. With only 10 physical qubits, the suggested $[[7,1,3]]$ stabiliser code displays 2.74 times less inaccuracy. Compared to normal distance-3 surface codes that utilise 25 qubits, this cuts overhead by 60%. Because they have a gate depth of 18, shallow syndrome extraction circuits can work in NISQ coherence windows of 20–100 gates. Machine learning-enhanced decoding gets 94.3% of the time right when it comes to classification. It can also fix faults in real time with a 12-microsecond inference delay that works with quantum processor cycle durations. Testing on IBM Quantum, IonQ, and Google Sycamore platforms shows that the framework works on superconducting qubit, trapped-ion, and simulated quantum computing architectures. A break-even performance occurs at 0.8% physical error rates, indicating feasible implementation routes on existing quantum hardware functioning at approximately 1% error rates. This work closes the important gap between theoretical quantum error correction and how to actually use it in NISQ, making it possible for variational quantum algorithms and quantum simulation applications to get a quantum computational advantage in the near future on current 50-100 qubit processors. The subsequent work may be augmented in the future: Extending the framework to encode 5-10 logical qubits with distributed decoding architectures and parallel syndrome processing for enhanced computational expressiveness and implementing online learning mechanisms enabling real-time decoder refinement responsive to time-varying noise characteristics and hardware drift.

References

1. P.W. Shor, Scheme for reducing decoherence in quantum computer memory, *Physical Review A* 52(4), pp. R2493-R2496, (1995) <https://doi.org/10.1103/PhysRevA.52.R2493>
2. A.M. Steane, Error correcting codes in quantum theory, *Physical Review Letters* 77(5) pp. 793-797, (1996), <https://doi.org/10.1103/PhysRevLett.77.793>
3. D. Gottesman, Stabilizer codes and quantum error correction, Ph.D. Thesis, California Institute of Technology (1997), <https://arxiv.org/abs/quant-ph/9705052>
4. A.Y. Kitaev, Fault-tolerant quantum computation by anyons, *Annals of Physics* 303(1), pp.2-30, (1997), [https://doi.org/10.1016/S0003-4916\(02\)00018-0](https://doi.org/10.1016/S0003-4916(02)00018-0)
5. E. Dennis, A. Kitaev, A. Landahl, J. Preskill, Topological quantum memory, *Journal of Mathematical Physics* 43(9), 4452-4505, (2002), <https://doi.org/10.1063/1.1499754>
6. A.G. Fowler, M. Mariantoni, J.M. Martinis, A.N. Cleland, Surface codes: Towards practical large-scale quantum computation, *Physical Review A* 86(3), 032324, (2012), <https://doi.org/10.1103/PhysRevA.86.032324>
7. C. Chamberland, A.W. Cross, Fault-tolerant magic state preparation with flag qubits, *Quantum* 3, 143, (2019), <https://doi.org/10.22331/q-2019-05-20-143>
8. R. Chao, B.W. Reichardt, Quantum error correction with only two extra qubits, *Physical Review Letters* 121(5), 050502, (2018), <https://doi.org/10.1103/PhysRevLett.121.050502>
9. P. Aliferis, J. Preskill, Fault-tolerant quantum computation against biased noise, *Physical Review A* 78(5), 052331, (2008), <https://doi.org/10.1103/PhysRevA.78.052331>
10. A. Kandala, K. Temme, A.D. Córcoles, A. Mezzacapo, J.M. Chow, J.M. Gambetta, Error mitigation extends the computational reach of a noisy quantum processor, *Nature*, 567(7749), 491-495, (2019), <https://doi.org/10.1038/s41586-019-1040-7>
11. K. Temme, S. Bravyi, J.M. Gambetta, Error mitigation for short-depth quantum circuits, *Physical Review Letters*, 119(18), 180509, (2017), <https://doi.org/10.1103/PhysRevLett.119.180509>
12. Y. Li, S.C. Benjamin, Efficient variational quantum simulator incorporating active error minimization, *Physical Review X* 7(2), 021050, (2017), <https://doi.org/10.1103/PhysRevX.7.021050>
13. G. Torlai, R.G. Melko, Neural decoder for topological codes, *Physical Review Letters*, 119(3), 030501, (2017), <https://doi.org/10.1103/PhysRevLett.119.030501>
14. P. Baireuther, T.E. O'Brien, B. Tarasinski, C.W.J. Beenakker, Machine-learning-assisted correction of correlated qubit errors in a topological code, *Quantum*, 2, 48, (2018), <https://doi.org/10.22331/q-2018-01-29-48>
15. H.P. Nautrup, N. Delfosse, V. Dunjko, H.J. Briegel, N. Friis, Optimizing quantum error correction codes with reinforcement learning, *Quantum*, 3, 215, (2019), <https://doi.org/10.22331/q-2019-12-16-215>
16. M.H. Abobeih, Y. Wang, J. Randall, S.J.H. Loenen, C.E. Bradley, M. Markham, D.J. Twitchen, B.M. Terhal, T.H. Taminiau, Fault-tolerant operation of a logical qubit in a diamond quantum processor, *Nature*, 606(7916), 884-889, (2022), <https://doi.org/10.1038/s41586-022-04819-6>
17. Z. Chen, K.J. Satzinger, J. Atalaya, A.N. Korotkov, et al., Exponential suppression of bit or phase errors with cyclic error correction, *Nature*, 595(7867), 383-387, (2021), <https://doi.org/10.1038/s41586-021-03588-y>
18. L. Egan, D.M. Debroy, C. Noel, A. Risinger, D. Zhu, D. Biswas, M. Newman, M. Li, K.R. Brown, M. Cetina, C. Monroe, Fault-tolerant control of an error-corrected qubit, *Nature*, 598(7880), 281-286, (2021), <https://doi.org/10.1038/s41586-021-03928-y>